Journal of Biomedical Optics

SPIEDigitalLibrary.org/jbo

# New noninvasive index for evaluation of the vascular age of healthy and sick people

Ilya Fine
Boris I. Kuznik
Alexander V. Kaminsky
Louis Shenkman
Evgeniya M. Kustovsjya
Olga G. Maximova

SPIE

# New noninvasive index for evaluation of the vascular age of healthy and sick people

**Ilya Fine,[a] Boris I. Kuznik,[b] Alexander V. Kaminsky,[a] Louis Shenkman,[c] Evgeniya M. Kustovsjya,[b] and Olga G. Maximova[b]**
[a]Elfi-Tech Ltd., Science Park, Rehovot, Israel
[b]Chita State Medical Academy, Chita, Russia
[c]Tel Aviv University, Sackler School of Medicine, Israel

**Abstract.** We conducted a study on 861 healthy and sick subjects and demonstrated that some calculated parameters based on measurement of the dynamic light scattering (DLS) signal from the finger correlate highly with chronological age ranging from 1.5 to 85 years old. Measurements of DLS signals were obtained during both occlusion and nonocclusion of blood flow in the finger. For the nonocclusion case we found that the low-frequency component of the DLS signal significantly correlates with the biological age while the high-frequency component of the DLS signal resembles the arterial pulse-wave and does correlate with age. However, the most prominent correlation between the DLS characteristics and age was noted with the stasis stage measurements. We propose that the observed age-related phenomena are caused by alterations in local blood viscosity and interactions of the endothelial cells with erythrocytes. Further, a new noninvasive index based on the age-related optical characteristics was introduced. This noninvasive index may be used as a research and diagnostic tool to examine the endothelial and thrombolytic properties of the vascular system.  [DOI: 10.1117/1.JBO.17.8.087002]

Keywords: coagulation; endothelial cells; dynamic light scattering; erythrocytes; pulse wave; blood viscosity.

Paper 12177P received Mar. 14, 2012; revised manuscript received Jul. 2, 2012; accepted for publication Jul. 3, 2012; published online Aug. 3, 2012; corrected Aug. 21, 2012.

## 1 Introduction

### 1.1 *Background*

Optical methods for assessment of physiological variables of the blood are used widely in medicine. However, very few of the existing methods can yield substantial information regarding the intravascular movement of the red blood cells (RBC) in the peripheral blood vessels. This information is required for in vivo assessment of hemostatic processes and endothelial functioning. It is well known that the vascular wall plays a key role in coagulation and fibrinolysis.[1–3] The risk of intravascular clotting may be enhanced by an altered balance between these two processes in the vascular wall. Two factors that can affect the functioning of this system are natural aging and pathological processes, both of which may impair this dynamic equilibrium.

There was an earlier report on the use of dynamic light scattering (DLS) for studying hemodynamic and vascular parameters at different physiological and pathophysiological conditions in vivo.[4,5] In our previous studies[6–8] we measured intravascular mobility of RBC as a natural marker of the effective viscosity of the blood plasma in close proximity to the vascular wall. For this end, we utilized DLS[9] for measurement of the RBC diffusion coefficient under the condition of intermittent stasis. Such a stasis condition is induced by oversystolic occlusion at the measurement location. We used the finger root as a convenient site to implement this technique. In the so-called occlusion spectroscopy,[10] oversystolic pressure is applied to the finger root in order to create a state of temporary blood flow cessation. During the occlusion stage the optical response is measured under the pressure cuff or at any other downstream location.

It was unequivocally shown by using a standard light transmission and reflection technique[10] that the arterial blood being squeezed under the high-pressure cuff is responsible for the manifestation of the time-dependent optical response. More specifically, during the stage of blood flow cessation, the light reflection or transmission signals tend gradually increase in time. These changes can be expressed in terms of the scattering and absorption coefficients of the RBCs. The scattering is associated with the size of the RBCs or RBC aggregations and the absorption coefficient is dependent on the hemoglobin oxygenation level. However, both absorption- and scattering-related parameters provide no information regarding the movement of the RBCs during the stasis stage. Thus, in order to comprehend the dynamic processes occurring during the intravascular blood stasis, an additional examination technique has to be introduced.

The DLS approach is a powerful tool to determine the statistical characteristics of moving scatterers.[9,11,12] The origin of the DLS signal lies in the addition of a number of randomly phased contributions of the reflected waves of the coherent light. The DLS signal is characterized by the temporal pattern created by an interference of the scattered light by an ensemble of the moving scatterers. This pattern moves as the scattering particles move, resulting in the fluctuations of the measured signal. The intensity fluctuation time scale is determined by the time that the scatterer has traveled the distance of one wavelength. Thus, the information about the movement of the scatterers is encrypted in time domain function.

Address all correspondence to: Ilya Fine, Elfi-Tech Ltd., Science Park, Rehovot, Israel. Tel: 972-89477140; Fax: 972-89477142; E-mail: ilyafine@elfi-tech.com.

0091-3286/2012/$25.00 © 2012 SPIE

In our previous research[7] we suggested the use of DLS to characterize the RBC interaction with the vessels' walls during the stasis stage. In this research we compared the characteristics of the signals obtained from the occluded blood to the characteristics of the signals obtained from the freely flowing blood at the same measurement site. For further analysis we expressed the DLS signal in terms of the power spectrum. Out initial suggestion was that the low-frequency component of DLS signal is contributed mainly by the slowly moving RBCs. These particles are located in close vicinity to the vascular walls and their mobility is strongly affected by the endothelium-RBC interaction and local blood plasma viscosity. We assumed, therefore, that the low-frequency component of the DLS signal will resemble the DLS signal obtained during stasis.

In this way, the DLS methodology both for freely moving RBCs and for RBCs suspended in the occluded volume was applied to elaborate the primary goal of this study, namely to make an assessment of the interaction between the RBCs and vascular walls. The adhesion of RBCs to vascular endothelium is thought to play an important role in the blood circulation and coagulation process.[13] Another important fact is that the very ability of the endothelium to respond and to ensure the best rheological performances decreases with age.[14] Thus, the function of the endothelium may serve as an important age-related marker. In current medical and biological studies several noninvasive age-related vascular markers are employed. For example, intima-media thickness is associated with the risk of atherosclerosis and can be examined by imaging techniques.[15] Additionally, a biomechanically derived age-related biomarker characterizes the arterial stiffness in terms of pulse wave velocity.[16] In this study we introduce a methodology that may provide the research with an additional vascular marker that is closely associated with endothelium function in vivo.

### 1.2 *Theoretical Consideration*

We consider an ensemble of light-scattering RBC particles, which are illuminated by the coherent light with the amplitude $E_0$. The scattered signal is measured by the detector that is located in close vicinity to the light source. The amplitude of the measured reflected signal is summed by the $N$ amplitudes of scattered light by all particles in the measured volume.[11]

$$E_m = E_0 \cdot \sum_{i=1}^{N} \exp[i \cdot q \cdot r_i(t)], \tag{1}$$

where $E_0$ is the field amplitude, and $r_j(t)$ is the position vector of the $j$'th particle at time $t$.

The measured intensity is defined by

$$I(t) \approx E_m \cdot E_m^*. \tag{2}$$

The difference $q$ between the wave vectors of scattered and incident wave is given by[12]

$$q = 4 \cdot \pi \cdot n \cdot \sin(\theta/2)/\lambda, \tag{3}$$

where $\theta$ is the scattering angle, $n$ is refractive index of the plasma, and $\lambda$ is the wavelength.

As has been shown in Ref. 7 for the measurement system where the detector and light source are located very closely, the summed-up amplitude of the measured signal is mostly contributed by the photons that are backscattered ($\theta = 180$ deg) from the RBC. Indeed, the light that is scattered from the RBCs is highly anisotropic and most of the radiation is scattered into the forward direction around a very small angle (less than 4 deg). When the distance between the detector and the light source is significantly larger than the mean free path of the scattered light, a significant part of the scattered photons can be redirected into the back hemisphere by a chain of the single forward scattering events (multiple scattering). However, when the detector is located in close vicinity to the light source, only the backscattered photons can return to their exit point. We consider the case that resembles our measurement geometry, where the backscattering component is dominant, meaning we can set in Eq. (3) $\theta = \pi$ making $q = 4\pi n/\lambda$.

We are going to consider two different modes of the movement of the RBCs: the stasis mode and the mode of laminar blood flow. In the first case we are interested in the random drifting of RBCs suspended in blood plasma, where the most widely used characteristic of the system is given by the diffusion coefficient, $D_B$. For Brownian motion, this characteristic is described by the Einstein-Stokes equation:[9]

$$D_B = K_B \cdot T/(3 \cdot \pi \cdot \eta \cdot d), \tag{4}$$

where $T$ is the temperature of the suspension, $K_B$ is the Boltzmann constant, $\eta$—viscosity of plasma, and d is the characteristic dimension of the particle.

Under the nonstasis condition, the RBCs are continually moving along the length of each blood vessel. In this case we are interested in the relative motion of the moving particles driven by the shear forces of the bloodstream.

If $T$ is the measurement time interval, then the normalized autocorrelation function is derived from the intensity fluctuations by[12]

$$\mathrm{ACF}(\tau) = \int_0^T I(t) \cdot I(t+\tau) \cdot \mathrm{d}t \Big/ \int_0^T I(t)^2 \cdot \mathrm{d}t. \tag{5}$$

In the simplified case, where only one parameter describes the system, the ACF exponentially decays[9] with characteristic time $t_c$:

$$\mathrm{ACF}(t) \approx \exp(-\tau/t_c). \tag{6}$$

For the particle in Brownian motion, this characteristic time is dependent[11] on the diffusion coefficient and optical parameter $q$:

$$t_c = 1/(2 \cdot D_B \cdot q^2). \tag{7}$$

Another extreme situation we examine is the blood flow in the vessels. In this case the ACF can be expressed in terms of the variance of the velocity difference across the vessel.[11] This parameter is dependent on the velocity of the blood flow, radius of the vessel, and viscosity of the blood and plasma. The decay constant $t_c$ in Eq. (7) will be approximated by[11]

$$t_c \approx \left(q \cdot \left\langle \sqrt{\Delta V^2} \right\rangle\right)^{-1}. \tag{8}$$

For the cylindrical vessel with radius $R$, the velocity profile $V(r,t)$ can be approximated by[17]

$$V(r,t) = V_{\max} \cdot \left[1 - \left(\frac{r}{R}\right)^K\right] \cdot \phi(t), \tag{9}$$

where $r$ is the distance from the central of the cross session of the vessel, $\varphi(t)$ is a periodic function of time, phase related with respect to the cardiac cycle, $K$—defines the degree of blunting or how close the velocity profile to the parabolic form. For small arterioles $K$ usually varies from 2 to 4 for different kinds and sizes of vessels. The exact form of the velocity profile will define $t_c$ . Since different geometrical locations in the vessels will contribute differently to the measured signal, the ACF in Eq. (8) represents the contribution from the geometrical center of points with equal variance of the differences of the velocity. The practically measured values of the DLS signal will include the components from different points and vessels and cannot be represented by a single exponential decay.

The above considerations yield the conclusion that the DLS signal in vivo can be used for the estimation of the motion patterns of the RBC movements for both Brownian movement and shear rate characteristics, while the underlying physical mechanisms responsible for the decay of the autocorrelation function are very different for each case.

In order to calculate the ACF and to decompose this function as a sum of a few exponents, a statistically significant number of measurement points have to be accumulated. Practically, in vivo measurement conditions are strongly affected by motion artifacts and other dynamic changes inducing time limitations into the available sampling interval. Therefore, a more robust, albeit less explicit characteristic has to be used for the analysis of the results. For this end we used the power spectrum characteristics.

The spectral density related to the ACF can be given by[12]

$$P(t_c,\omega) \approx \int_{-\infty}^{\infty} \mathrm{ACF}(\tau, t_c) \cdot \exp(i \cdot \omega \cdot \tau) \cdot \mathrm{d}\tau. \qquad (10)$$

The very robust measurable characteristic of the DLS signal is the variance (VAR) of the detected intensity fluctuation. This parameter gives the highest signal-to-noise ratio and relates to the spectral density through Eq. (10). We defined therefore the integral characteristics by

$$\mathrm{VAR}(t_c) \approx \int P(\omega) \cdot \mathrm{d}\omega. \qquad (11)$$

From Eqs. (8) and (10) it can be seen that VAR is a function of the sought decay time or times, related to the RBC motion characteristics. The measured value VAR from Eq. (11) is, therefore, an indirect integral characteristic of the $t_c$.

In order to reduce sensitivity to the motion artifacts in our measurement system, the high-pass analog filtration was implemented. In addition, in our further analysis we utilized the digital filters with different response functions. By taking into consideration these filters we defined $S$ by:

$$S(t_c) = \int P(\omega) \cdot \zeta(\omega) \cdot \psi(\omega) \cdot \mathrm{d}\omega, \qquad (12)$$

where $\psi(\omega)$ is spectral response of the analog instrumental filter $\zeta(\omega)$ is the spectral response of the digital filter.

The value $S(t_c)$ was found to be a very stable and reproducible in vivo parameter. According to the measurement mode (occlusion or free flow), and according to the frequency spectral function $\zeta(\omega)$ a few different kinds of the modified functions $S$ can be defined.

We designated $S*(\mathrm{HF})$ for the $S$ from Eq. (12) where $\zeta(\omega)$ is the high-pass filter response and $S*(\mathrm{LF})$ for the low-pass filter response. For $S*(\mathrm{LF})$ $\zeta(\omega)$ was defined by the low-pass Butterworth filter of 100 and 500 Hz high-pass Butterworth filter was imposed for the $S*(\mathrm{HF})$.

In order to make the $S$ characteristics usable by clinicians and biologists, we introduced a new index, SKF, by converting the $S$ values into parameters with very specific biological meaning. Based on a significant correlation that has been found in our study between $S$ and the chronological age, we defined SKF by

$$\mathrm{SKF}(t_c) = \alpha_1 + \beta_1 \cdot \langle S(t_c) \rangle, \qquad (13)$$

where $\alpha_1$ and $\beta_1$ are the calibration constants, and $S$ from Eq. (12) is averaged over a predetermined asymptotic interval of the occlusion stage. The constants $\alpha_1$ and $\beta_1$ were derived from the linear best fit of the measured $S$ and the logarithm of the subject's age in the years (AG). $S$ for the occlusion case is found from Eq. (12) where $\zeta = 1$. Thus, SKF can be considered as an optical equivalent of the biological age in the logarithmic scale.

We also used SKF* for the nonoccluded blood measurement. The averaging is over all nonoccluding intervals:

$$\mathrm{SKF}^* = \alpha_1 + \beta_1 \cdot \langle S^* \rangle. \qquad (14)$$

We used SKF$*$(HP), and SKF$*$(LP) where $S*(\mathrm{HP})$, and $S*(\mathrm{LP})$, correspondingly, are used instead of $S$ in Eq. (12).

## 2 Measurement System

The *in vivo* DLS measurement system (ELFI-TECH3)[7] consists of three parts: the probe unit, the acquisition and processing system, and the electronic and control unit. The probe unit includes the 850-nm vertical cavity surface emitting laser, the pressurizing assembly, detector, and amplifier. The pressure cuff is controlled by the electronic unit. The laser and the detector are located under the cuff. The distance between them is 2 mm. The laser is operated in CW mode. The signal acquisition is done with the sampling frequency of 16 KHz with the ADC resolution of 12 bit. The digitized signal is saved in memory of the processor for further offline analysis.

The measurement process starts when, by means of a pneumatic cuff, the oversystolic pressure is applied and blood flow cessation for the predetermined time interval (Fig. 1).

The stasis-related DLS signal was measured for 20 s during the occlusion session. At the next measurement session the system performed automatic measurement without occlusion

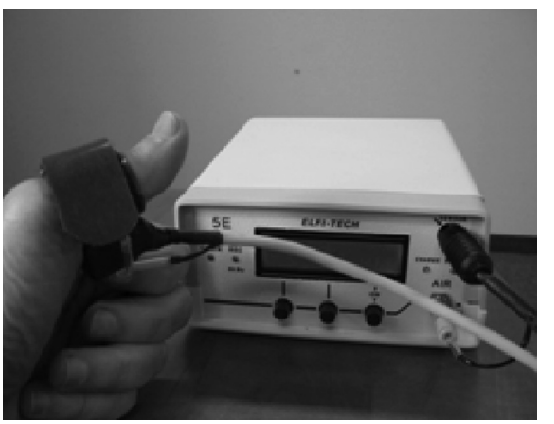

**Fig. 1** Measurement system where the finger is held at the measurement position and a pressure cuff is wrapped around the finger.

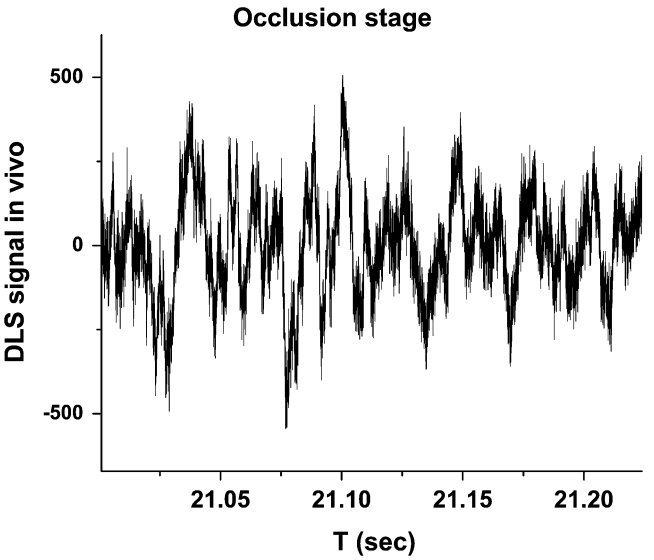


**Fig. 2** Typical DLS signal measured in vivo during the occlusion stage.

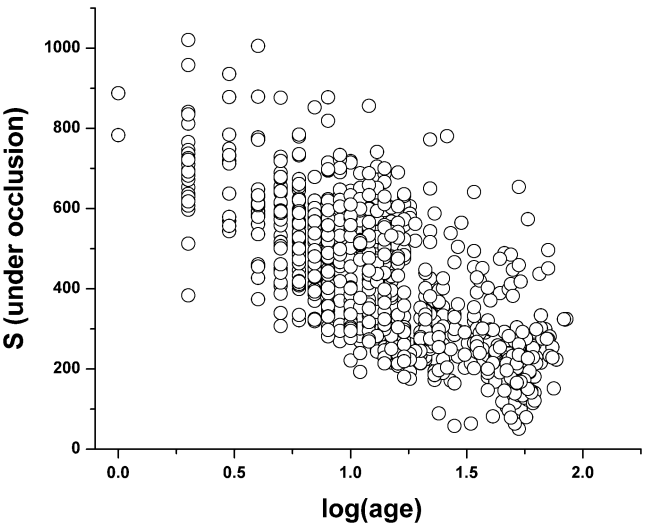


**Fig. 3** Typical $S$ under occlusion as function of age.

for 15 s. The results of this measurement session were used for different assessments of the characteristics of the flowing blood. A typical raw data example that has been measured for 1 s during the stasis session is shown in Fig. 2. The time-dependent pattern of the intensity fluctuations is originated by the intravascular movement of the RBCs.

## 3 Methods

Our study was conducted on 861 healthy and sick subjects (male and female) ranging in age from 1.5 to 85 years. The research protocol was approved by the local Helsinki Committee. All patients were tested with the ELFI-3 device. Measurements were obtained during sitting or supine position. The sensor was fixed at the finger base. At the beginning of the measurement the pneumatic cuff was inflated to 280 mm Hg, occluding all the blood vessels under the cuff and causing the stasis stage. The cuff was kept inflated for 20 s and then the pressure in the pneumatic cuff was released. The DLS signal was measured during this entire interval and stored as a file. Several seconds after the release of the pressure cuff, the next measurement session of 15 s was started, and the resulting signals were detected and stored. All together five measurement cycles were performed for each patient, two occlusion and three nonocclusion intervals.

The measurement results between the 16 and 20 s of the stasis stage were used for the determination of the power spectrum and $S$. The SKF indexes were calculated from Eqs. (13) and (14) where $S$ values were averaged overall measurement for a given patient.

## 4 Results and Discussion

Initially we analyzed the signals obtained during the occlusion stage. We chose the time $T$ in Eq. (5) to be long enough to make the statistical analysis reliable. In our processing we took $T = 4$ s for each point of the occlusion stage.

We found that the $S$ value was highly negatively correlated with the logarithm of the chronological age (Fig. 3). That is, the higher the age, the lower the $S$ value.

The coefficients $\alpha_1$ and $\beta_1$ in Eq. (13) were adjusted for all data sets by using an assumption of the linear relationship

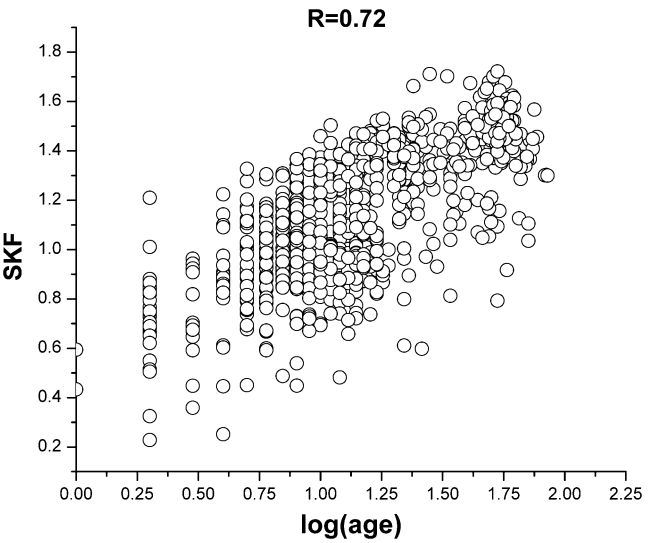


**Fig. 4** SKF as function of age.

between $S$ and the logarithm of the age. Then the SKF index was calculated by using Eq. (14). In Fig. 4 SKF is shown as a function of log(age). The same results can be represented in terms of average $S$, according to the age groups. We represent the result in terms of $S$, to show a tendency of exponential decay of $S$ as a function of age (Fig. 5).

The next results address the measurements sessions without occlusions. Figure 6 depicts the $S*(\mathrm{LF})$ behavior during the 20-s measurement session. The signal fluctuates without any noticeable pattern. However, when the same recorded signal was passed through the high pass filter and $S*(\mathrm{HF})$ was calculated, a typical pulsatile signal was observed, quite resembling the PPG pattern of the flowing blood (Fig. 7).

The next example (Fig. 8) illustrates on the same plot how the $S*(\mathrm{HF})$ and S*(LF) respond to the occlusion event. In this 60-s experiment the occlusion was applied after the 10 s. We can see that the $S*(\mathrm{HF})$ (dashed line) reveals the pulsatile pattern at the beginning of the measurement and immediately after the occlusion event $t$ this parameter drops without any significant variation until the end of the occlusion. At the same time,

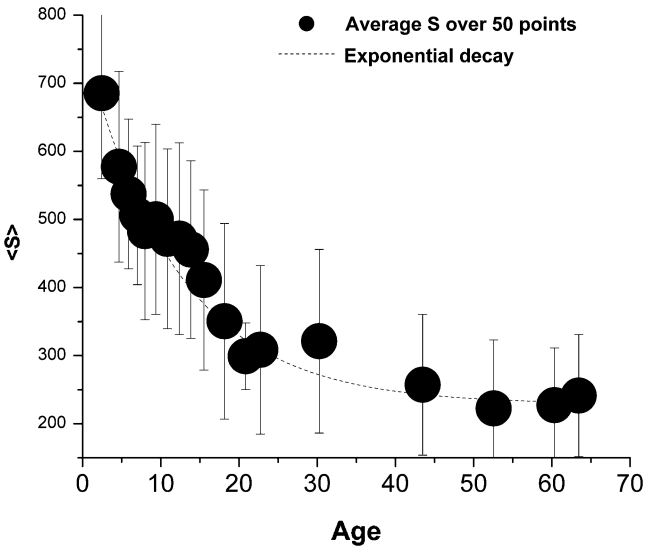


**Fig. 5** $S$ value averaged over every 50 patients as function of age (in years) resembles the exponential decay.

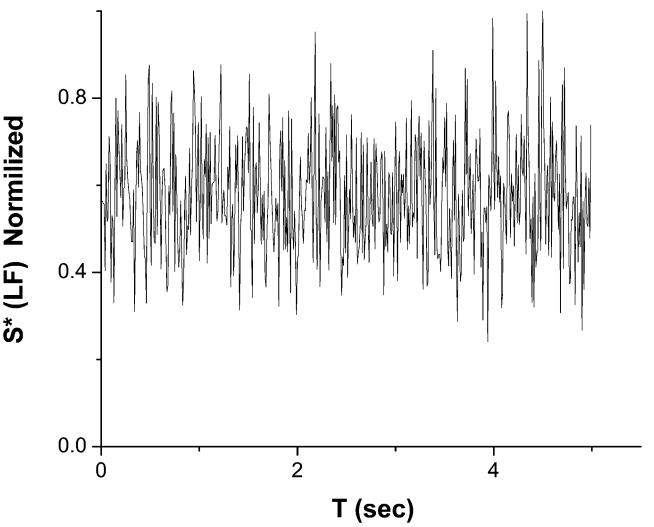


**Fig. 6** $S*(\mathrm{LF})$ during the measurement. No occlusion is applied.

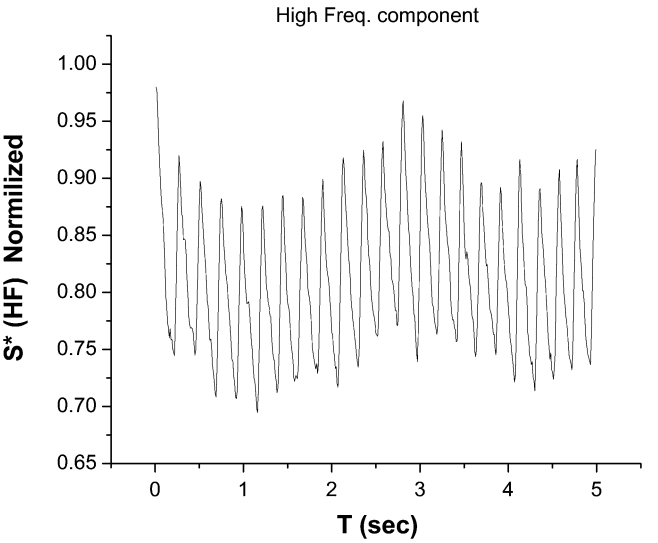


**Fig. 7** $S*(\mathrm{HF})$ during 20 s of the measurement. No occlusion was applied.

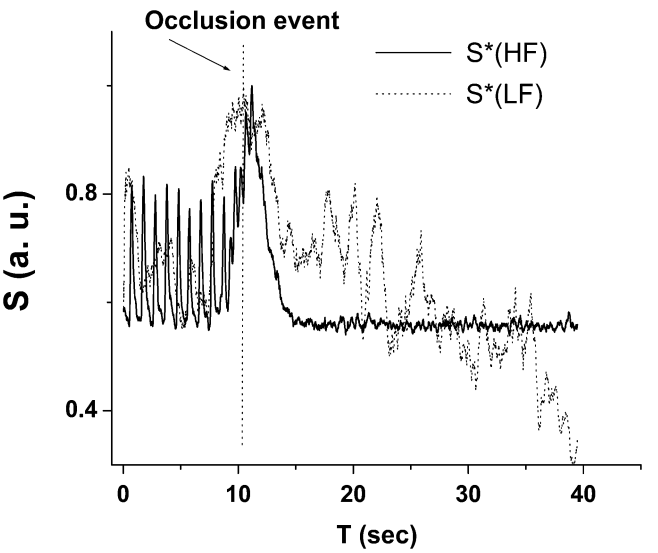


**Fig. 8** $S*(\mathrm{HF})$ and $S*(\mathrm{LF})$ during the 1 min monitoring. At the 10th second, occlusion was applied.

the $S*(\mathrm{LF})$ component gradually decreases during the occlusion.

What is very remarkable is that the sudden blood flow cessation does not immediately affect the optical response characteristic $S*(\mathrm{LF})$, indicating that this signal is associated with the very slowly moving RBCs and is not associated with the flowing blood. This observation led us to check if the $S*(\mathrm{LF})$ reveals the similar properties with regard to the age, as the $S$ value derived from the occlusion measurement.

Figures 9 and 10 show the dependence of the average SKF$*$(LF) Eq. (9) and SKF$*$(HF) Eq. (10) being calculated from Eq. (14). It can be seen that the low-frequency component of the signal reveals a very significant dependence on the age. Actually, as seen in Fig. 11, there is a strong correlation between the SKF measured during the occlusion and SKF$*$(LF) derived from the stage of free blood flow.

While the SKF changes rapidly for ages below 30, the high-frequency component $S*(\mathrm{HF})$ is not sensitive to ages below 30 and has a slight tendency to increase with higher ages. This can be explained by the fact that the peripheral blood flow velocity increased with age because of loss of elasticity of the vessels.

Helmbold et al.[18] demonstrated that two parameters, density of skin capillaries of the upper dermis plexus and pericytes to endothelial cell ratio (PC:EC), fall exponentially with age, very similarly to the SKF age behavior as is presented in Fig. 5. It is, however, difficult to assume that the density of the capillaries is somehow related to the optical measurements we carried out. During the very high occlusion pressure that was applied on the skin, it is most likely that all capillary and venous blood was expelled from the measurement site.

So we remained with the PC:EC ratio exponential falling with age. Pericytes are wrapped around precapillary arterioles, around blood capillaries and postcapillary venules. Interactions between endothelial cells and pericytes in the blood vessel wall recently have been identified as an important process in the regulation of vascular function.[18] Pericytes play an important role in

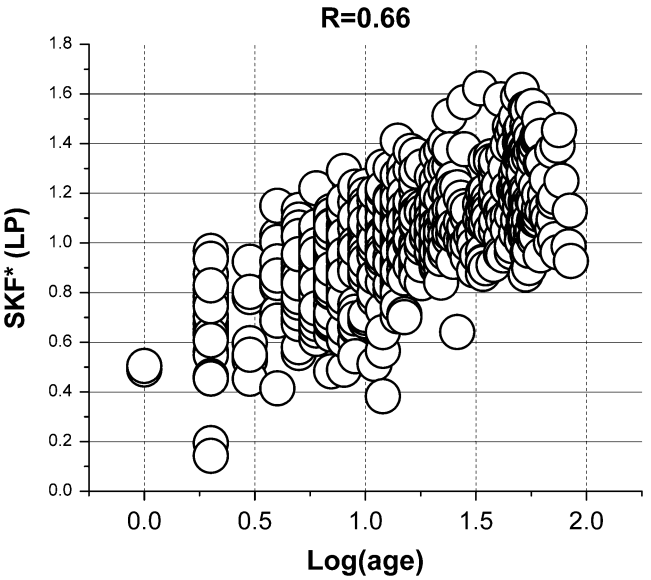


**Fig. 9** SKF ∗ (LF) as a function of age.

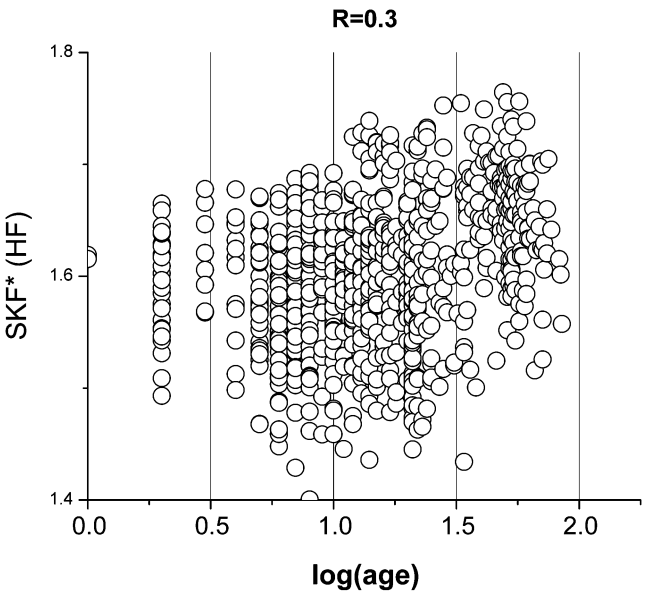


**Fig. 10** SKF ∗ (HF) as a function of age.

maintenance of hemostasis through their interaction with the endothelial cells. Both procoagulant and fibrinolytic proteins are synthesized by endothelial cells. Thus, we assume that local blood viscosity and RBC interaction with blood vessels is driven by endothelial functioning and different stages of hemostasis. These processes are manifested through the mobility of the RBCs that are located near the vessel walls. Taken together, these mechanisms are responsible for the characteristics of the slowly moving RBCs.

Indeed, Fig. 8 shows that the DLS signal associated with the RBCs' movement is very strong, specifically during the first 10 s after the occlusion is applied. In due course the DLS signal gradually decreases, indicating that the RBCs' mean free path decreases. Since under occlusion condition the blood flow pressure wave cannot affect the RBC movement, only very local mechanisms related to the plasma and vessels wall properties are

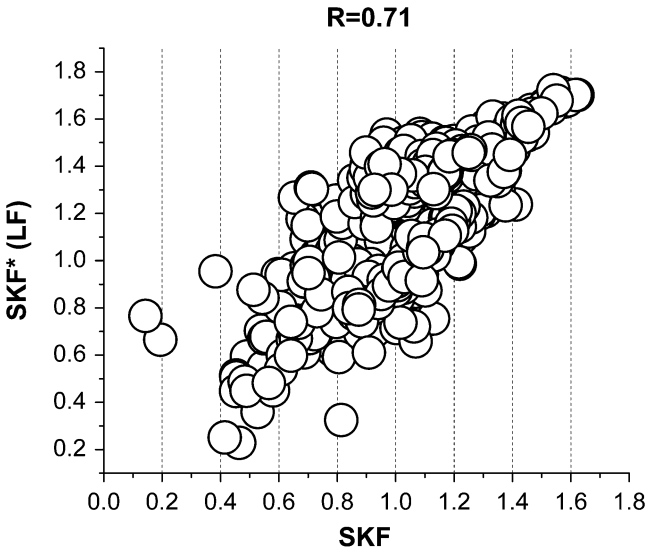


**Fig. 11** SKF ∗ (LF) (no occlusion) as a function of SKF (occlusion).

responsible for the RBCs' movement. When blood flows freely through the vessels, the hemorheological parameters are responsible for the RBC flow. None of these factors are directly related to the age-related phenomena, however, and even during flow conditions there is a layer of RBCs that creates unmediated contact with the blood vessel walls.

At very close vicinity to the vascular wall the laminar velocity of the RBCs is negligible, and they are participating in the movement that is driven by the same parameters as for the RBC in the occluded vessels. The low-frequency component of the DLS signal is originated by these slow-moving RBCs. Therefore, we observe a strong correlation between the DLS signal during the occlusion stage and the DLS low-frequency component. In both cases the slow movement of the RBC is affected by the combined action of the endothelial cells and thrombolytic events.

The analysis of the variation of the values of SKF provides us with some insights into the physiological interpretation of this parameter. The highest level of SKF corresponds to the lowest level of $S$. As seen from Eqs. (12) and (14), the high $S$ value indicative to the fast movement of the RBCs. The found correlation between the $S$ and chronological age implies that the intravascular near-wall movement of the RBCs gradually decays with age. This can be explained by increased interaction forces between the RBCs and vascular wall. Therefore, the SKF index provides a measure of the strength of the interaction between the vascular wall and the RBCs. This index is expressed in terms of the chronological age, so the higher the SKF, the higher is the resistance to the free movement of the RBCs.

When seeking the clinical implications of these discovered phenomena, it should be noted that the endothelial cells are the major site responsible for the expression of tissue factor, anticoagulants, fibrinolytic factors, and inhibitors of fibrinolysis.[1] Therefore the mobility of RBCs near the blood vessel wall will be strongly affected by hemostasis-related processes. The shift toward hyper-coagulativity and less efficient functioning of endothelial cells is also a natural process occurring during aging.

We, therefore, conclude that the newly introduced SKF index enables evaluation of functional indices of the vascular system and the hemostasis system from infancy to advanced age. The

proposed methodology may be tested for the identification of different diseases, monitoring of coagulation status, and anticoagulation drug management.

## References


1. B. I. Kuznik, "Cellular and molecular mechanisms of hemostatic system regulation by norm and pathology," Vol. 828, Chita Express, Chita, (2010).
2. B. I. Kuznik, N. W. Vasilyev, and N. N. Tsybikov, "Immunogenesis, hemostasis and nonspecific resistance of the organism," p. 315, Meditsina, Moscow (1989).
3. B. P. Boucher et al., "LRP: role in vascular wall integrity and protection from atherosclerosis," *Science* **300**(5617), 329–332 (2003).
4. V. Kalchenko et al., "In vivo dynamic light scattering microscopy of tumour blood vessels," *J. Microsc.* **228**(2), 118–122 (2007).
5. V. Kalchenko et al., "In vivo dynamic light scattering imaging of blood coagulation," *J. Biomed. Opt.* **12**(5), 052002 (2007).
6. I. Fine and A. Kaminsky, "Speckle-based measurement of the light scattering by red blood cells in vivo," *Proc. SPIE* **7898**, 78980A (2011).
7. I. Fine et al., "A non-invasive method for the assessment of hemostasis in vivo by using dynamic light scattering," *Laser Phys.* **22**(2), 1–7 (2012).
8. B. I. Kuznik, I. W. Fine, and A. V. Kaminsky, "Non-invasive method of the examination of the hemostatis system," *Bull. Exp. Biol. Med.* **151**(5), 655–657 (2011).
9. B. J. Berne and R. Pecora, *Dynamic Light Scattering with Applications to Chemistry, Biology, and Physics*, Dover Publications, Inc., Mineola, NY (2000).
10. I. Fine, B. Fichte, and L. D. Shvartsman, "Occlusion Spectroscopy as a new paradigm for non-invasive blood measurements," *Proc. SPIE* **4263**, 122–130 (2001).
11. W. I. Goldberg, "Dynamic light scattering," *Am. J. Phys.* **67**(12), 1152–1160 (1999).
12. B. Chu, *Laser Light Scattering*, Dover Publications, Inc., Mineola, NY (2007).
13. S. Yedgar, D. K. Kaul, and G. Barshtein, "RBC adhesion to vascular endothelial cells: more potent than RBC aggregation in inducing disorders," *Microcirculation* **15**(7), 581–583 (2008).
14. R. P. Brandes, I. Fleming, and R. Busse, "Endothelial aging," *Cardiovasc. Res.* **66**(2), 286–294 (2005).
15. T. Jogestrand, O. Eiken, and J. Nowak, "Relation between the elastic properties and intima-media thickness of the common carotid artery," *Clin. Physiol. Funct. Imaging* **23**(3), 134–137 (2003).
16. S. Shibata and B. D. Levine, "Effect of exercise training on biologic vascular age in healthy seniors," *Am. J. Physiol. Heart Circ. Physiol.* **302**(6), H1340–H1346 (2012).
17. A. S. Popel, "Microcirculation and hemorheology," *Annu. Rev. Fluid. Mech.* **37**, 43–69 (2005).
18. P. Helmbold et al., "Detection of a physiological juvenile phase and the central role of pericytes in human dermal microvascular aging," *Dermatology* **126**(6), 1419–1421 (2006).